The small RNA SgrS controls sugar–phosphate accumulation by regulating multiple PTS genes

Jennifer B. Rice and Carin K. Vanderpool*

Department of Microbiology, University of Illinois at Urbana-Champaign, Urbana, IL 61801, USA

ABSTRACT

A number of bacterial small RNAs (sRNAs) act as global regulators of stress responses by controlling expression of multiple genes. The sRNA SgrS is expressed in response to glucose–phosphate stress, a condition associated with disruption of glycolytic flux and accumulation of sugar–phosphates. SgrS has been shown to stimulate degradation of the *ptsG* mRNA, encoding the major glucose transporter. This study demonstrates that SgrS regulates the genes encoding the mannose and secondary glucose transporter, *manXYZ*. Analysis of *manXYZ* mRNA stability and translation in the presence and absence of SgrS indicate that *manXYZ* is regulated by SgrS under stress conditions and when SgrS is ectopically expressed. *In vitro* footprinting and *in vivo* mutational analyses showed that SgrS base pairs with *manXYZ* within the *manX* coding sequence to prevent *manX* translation. Regulation of *manX* did not require the RNase E degradosome complex, suggesting that the primary mechanism of regulation is translational. An *Escherichia coli ptsG* mutant strain that is *manXYZ*⁺ experiences stress when exposed to the glucose analogs α-methyl glucoside or 2-deoxyglucose. A *ptsG manXYZ* double mutant is resistant to the stress, indicating that PTS transporters encoded by both SgrS targets are involved in taking up substrates that cause stress.

INTRODUCTION

Trans-acting bacterial small RNAs (sRNAs) are encoded at chromosomal sites distal to those of their target mRNAs. These sRNAs act by base pairing with mRNAs and either positively or negatively affect translation or mRNA stability (1). For enterobacterial sRNAs, pairing requires the RNA chaperone, Hfq, which is thought to stimulate base pairing interactions by remodeling RNA structures and by increasing local concentrations of the sRNA and mRNA (2). The mechanism of negative regulation most commonly described involves base pairing between an sRNA and the 5′-untranslated region (UTR) of a target mRNA to block ribosome binding and inhibit translation (1). In numerous cases, the endoribonuclease RNase E and its associated proteins (collectively known as the degradosome) act on the sRNA–mRNA complex subsequent to translational repression. This results in coupled degradation of the sRNA and mRNA, rendering the regulation irreversible (1). There are other examples of sRNA-mediated negative regulation that do not adhere to the aforementioned model. The GcvB sRNA binds upstream of the ribosome binding sites of some target mRNAs and inhibits translation by blocking translational enhancer sites (3). The MicC sRNA binds within the coding region of one of its targets, *ompD* mRNA (4). The pairing occurs too far downstream to inhibit *ompD* translation initiation; instead, RNase E-dependent degradation is required for MicC-mediated repression of *ompD* (4). sRNA-mediated regulation of polycistronic transcripts can result in discoordinate regulation of genes in an operon. *galK* in the *galETKM* operon and *iscS* in the *iscRSUA* operon are negatively regulated by the sRNAs Spot 42 and RyhB, respectively (5,6). Both sRNAs bind to the ribosome binding sites of their target mRNAs to inhibit translation. Spot 42 inhibition of *galK* allows for translation of the upstream genes, *galET* (6) while RyhB inhibition of *iscS* causes degradation of the *iscSUA* portion of the transcript but generates a stable *iscR* transcript available for translation (5). Recently, coordinate regulation of the genes in an operon by the sRNA RsaE in *Staphylococcus aureus* was suggested by the identification of RsaE interactions with two different cistrons on a polycistronic transcript (7); no such example has been found for Hfq-dependent sRNAs. Since novel mechanisms of bacterial sRNA-mediated regulation are still being found, it is important to continue characterizing interactions of individual sRNA–mRNA pairs.

The transcription of many bacterial sRNAs is activated under specific stress conditions and their activities aid cells in recovery from those stresses (1). Transcription of the sRNA SgrS is activated under glucose–phosphate stress

*To whom correspondence should be addressed. Tel: +217 333 7033; Fax: +217 244 6697; Email: cvanderp@life.illinois.edu

conditions in *Escherichia coli* (8,9). These conditions arise if glycolysis is blocked, e.g. by a mutation in the *pgi* gene (so that glucose-6-phosphate accumulates) or if cells are exposed to a non-metabolizable glucose analog α-methylglucoside (αMG) (so that αMG-6-phosphate accumulates) (9,10). Growth of wild-type *E. coli* cells is transiently inhibited by this stress, while *sgrS* mutant cells are unable to continue growing under stress conditions (9). SgrS seems to promote growth recovery by two independent mechanisms. The first is a base pairing-dependent mechanism whereby SgrS pairs in an Hfq-dependent manner with sequences overlapping the ribosome binding site of *ptsG* mRNA. *ptsG* encodes the EIICB^{Glc} component of the Phosphoenolpyruvate Phosphotransferase System (PTS) glucose transporter in *E. coli*. Pairing between SgrS and *ptsG* mRNA prevents *ptsG* translation, thereby stopping synthesis of new glucose transporters (9,11). As part of this regulation, the SgrS–*ptsG* mRNA complex is degraded by the RNase E degradosome complex (12,13). In addition to the base pairing activity, SgrS encodes the small protein, SgrT. When SgrT is produced, it prevents glucose (or αMG) uptake by a mechanism independent of the base pairing activity (14). Likewise, the base pairing function of SgrS does not depend on production of the SgrT protein (14,15). The combination of these two SgrS functions was proposed to allow cells to stop sugar–phosphate accumulation and overcome growth inhibition. However, we recently determined that in stressed *E. coli* K12 cells, little SgrT is produced and the base pairing function appears to be primarily responsible for stress recovery (15).

Since several other characterized bacterial sRNAs target multiple mRNAs and the base pairing function of *E. coli* SgrS is required for rescue from glucose–phosphate stress, a preliminary microarray experiment was conducted to identify other putative SgrS targets. For this experiment, plasmid-borne SgrS was induced from a heterologous promoter for 5 min in an *sgrS* mutant host growing in rich medium. The transcriptomes of vector control and SgrS-expressing cells were compared and genes that were up- or downregulated were identified (our unpublished data). As expected, *ptsG* mRNA levels were decreased upon SgrS induction, as were levels of another mRNA encoding a PTS transporter, *manXYZ*. ManXYZ is a broad-substrate range sugar transporter that has been shown to transport mannose, glucose, 2-deoxyglucose, αMG, fructose, glucosamine, *N*-acetylglucosamine and trehelose (16–18). The *manX* gene encodes the EIIAB^{Man} cytoplasmic component of the transporter while *manY* and *manZ* encode the membrane components EIIC^{Man} and EIID^{Man}, respectively (18). The three genes are operonic and transcriptionally controlled in a manner similar to *ptsG* (18–20).

In this study, we show that the *manXYZ* polycistronic mRNA is negatively regulated by SgrS post-transcriptionally through a base pairing mechanism involving sequences downstream of the *manX* ribosome binding site. Translation of *manX* is inhibited and the entire *manXYZ* mRNA is degraded in an SgrS-dependent

manner under stress conditions. However, SgrS-mediated repression of *manX* translation does not require RNase E, which suggests a ribosome occlusion mechanism of translational inhibition. The physiological relevance of SgrS-mediated repression of *manXYZ* was demonstrated by the finding that EII^{Man} transports sugar analogs that induce the SgrS stress response.

MATERIALS AND METHODS

Strain and plasmid construction

The strains and plasmids used in this study are listed in Supplementary Table S1 and oligonucleotides are listed in Supplementary Table S2. Alleles were moved between strains by P1 transduction or inserted via lambda Red recombination (21). Translational LacZ fusions were constructed as described previously (22). Strain XL10 Gold (Stratagene) was used for the QuikChange Mutagenesis procedure. LacI^q (harbored in several strains, including JH111, Supplementary Table S1) was used to control expression from the P$_{lac}$ promoter.

The *manX′–′lacZ* translational fusion was created as described previously (22) using primers O-JH129/O-JH130 to fuse *lacZ* to the 34th codon of *manX*. The fusion was transduced into various backgrounds (see Supplementary Table S1) to create JH114, JH115, JH116, JH149, JH236 and JH255.

kan^R-Cp19-*manXYZ* was created by PCR-amplifying the kan^R-linked Cp19 promoter from JNB024 (N. Majdalani, J. Benhammou and S. Gottesman, unpublished results) chromosomal DNA using oligos containing *manX* homology (O-JH104/O-JH137). The resulting PCR product was recombined into NM200. kan^R-Cp19–*manXYZ* from this strain was transduced into wild-type (DJ480) and Δ*sgrS* (CS104) backgrounds to yield strains JH124 and JH125.

The kan^R-Cp19-*manX′–′lacZ* fusion was created as follows: kan^R-Cp19–*manXYZ* was transduced into NM200 to create JH131. pCP20 was used to flip out the kan^R cassette, resulting in strain JH136. Then the *manX′–′lacZ* fusion was created in the JH136 strain as described above.

Strains containing *manX* 5′ UTR mutations were created as follows: the *manX′–′lacZ* fusion was transduced into NM200 to create JH149. A tet^R-Cp19 PCR product generated using oligonucleotides O-JH161/O-JH175 was used as a PCR template to generate tet^R-Cp19–*manX* (O-JH173/O-JH163) and tet^R-Cp19–*manX*$_{30}$ (O-JH174/O-JH163) products. These PCR products were recombined into JH149 to create JH175 and JH181, respectively.

A *ptsG′–′lacZ* translational fusion (in strains JH169, JH172 and JH238) was created so that *lacZ* was fused in frame to *ptsG* codon 141 using methods described previously (22). Oligonucleotides O-JH153/O-JH154 were used to obtain the PCR product. The PtsG portion of the PtsG-LacZ fusion protein contains four transmembrane domains; LacZ remains in the cytoplasm. The tet^R-Cp19–*ptsG′–′lacZ* fusion was created by recombining a

tet^R-Cp19 cassette (amplified using oligonucleotides O-JH170/O-JH154) upstream of the *ptsG* 5′ UTR.

Chromosomal mutations in *manX* were made using the following method: a tet^R cassette (generated with oligonucleotides O-JH194/O-JH195) was inserted into *manX* so that nucleotides to be targeted for mutation were deleted. The resulting strain was named JH197. A PCR product (obtained using oligonucleotides O-JH199/O-JH130 or O-JH211/O-JH130 and strain JH113 as a template) containing the C143T or CAC to GUG *manX* mutations and a kan^R cassette at the desired *lacZ* fusion junction was recombined into JH197 creating JH208 and JH227, respectively. The *manX′–′lacZ* translational fusion was then constructed as described previously by flipping out the kan^R cassette and replacing with ′*lacZ* (22) to create JH212 and JH228. Another tet^R cassette was inserted into *manX* at a different site using a PCR product generated by primers O-JH220/O-JH195; the resulting strain was JH239. To make the strain JH240 containing the *manX* GTG to ATG mutation, a PCR product containing the mutation linked to a kan^R cassette (amplified using O-JH221/O-JH130) was recombined into JH239 and colonies were screened for tet sensitivity. The *manX′–′lacZ* translational fusion was constructed as described previously by flipping out the kan^R cassette and replacing with ′*lacZ* (22) to create JH241.

manX$_{Yp}$′–′*lacZ* and *manX*$_{Ecar}$′–′*lacZ* fusions were created by recombining a PCR product containing upstream and downstream homology to *E. coli manX* flanking the *Yersinia pestis* or *Erwinia carotovora manX* 5′ UTR and a kan^R marker into JH197. The kan^R marker was replaced by *lacZ* as described previously (22) to create JH232 (*manX*$_{Yp}$′–′*lacZ*) and JH264 (*manX*$_{Ecar}$′–′*lacZ*). The PCR products used to create these strains were derived by stitching two PCR products: (i) a product with homology upstream of *E. coli manX* and the *Y. pestis* or *E. carotovora manX* sequence and (ii) a product with homology to the *Y. pestis* or *E. carotovora manX* sequence linked to a kan^R marker. For *Y. pestis manX*, O-JH212/O-JH213 were used to create product 1. O-JH214/O-JH130 were used to create product 2. The same procedure was used to create the *E. carotovora manX′–′lacZ* fusion. The primers used were O-JH215/O-JH216, O-JH217/O-JH130 and O-JH215/O-JH130.

P$_{sgrS}$–*lacZ* was constructed by B. Hussain in our laboratory using the previously described 'Materials and Methods' section (9). P$_{sgrS}$ was amplified using primers O-BAH102 and O-CV142 containing *EcoR*I and *BamH*I sites. This product was cloned into pRS1553. The resulting fusion was recombined into the λ*att* site and the resulting strain was named BAH100. The original strain carrying Δ*ptsG::cat* was kindly provided by H. Aiba. Δ*ptsG::cat* was transduced into P$_{sgrS}$–*lacZ* (BAH100) to yield strain CS177. The original strain carrying Δ*manXYZ*::kan^R was obtained from Amos Oppenheimer. Δ*manXYZ*::kan^R was transduced into P$_{sgrS}$–*lacZ* (BAH100) and Δ*ptsG::cat* (CS177) backgrounds to yield strains CS178 and CS179.

Plasmid pBRJH19, containing the GUG to CAC mutation in SgrS, was created using the QuikChange Mutagenesis kit (Stratagene) with primers O-JH209/ O-JH210 and P$_{lac}$-*sgrS* (pLCV1) plasmid as template. Plasmid pBRJH23 was created using the QuikChange Mutagenesis kit with primer O-JH252 and P$_{lac}$-*sgrS10* (pBRJH19) as the template. Plasmid pBRJH26, containing the G168A mutation, was created using the QuikChange Mutagenesis kit with primer O-JH260 and the pLCV1 plasmid as a template.

Media and reagents

Bacteria were cultured in LB medium or on LB agar plates at 37°C unless otherwise noted. TB medium (Bacto Tryptone, BD) was used for β-galactosidase assays. Media were supplemented with 100 μg/ml ampicillin where indicated. IPTG was used at a concentration of 0.1 mM for induction of P$_{lac}$-*sgrS*. MOPS (morpholine-propanesulfonic acid) rich defined medium (Teknova) with 0.2% mannose as a carbon source was used for culturing cells for RNA extraction for 5′ RACE. MacConkey indicator plates supplemented with 1% lactose were used to measure P$_{sgrS}$–*lacZ* activity.

β-galactosidase assays

Strains containing translational fusions were grown overnight in TB medium and subcultured 1:200 to fresh medium. Cultures were grown to an OD$_{600}$ ∼0.1 at which time 0.5% αMG or 0.1 mM IPTG was added to cells. Samples were taken at times indicated and assayed for β-galactosidase activity as described previously (23). Activities (in Miller Units) were normalized to Δ*sgrS* or empty vector control to give the percentage relative activity for experimental samples.

RNA extraction and northern blot analysis

Strains were grown in LB medium to OD$_{600}$ ∼0.5 and exposed to 0.5% αMG. RNA was extracted at times indicated by the hot phenol method as described previously (24). The RNA concentration was determined spectrophotometrically. Fifteen microgram of total RNA was used for electrophoresis and run on a 1.2% agarose gel alongside the Millenium Marker (Ambion) at 90 V for ∼1.5 h. RNA was transferred to a membrane as described previously (25). Prehybridization was performed in ULTRAhyb (Ambion) solution at 42°C for at least 45 min. Blots were subsequently probed overnight with a 5′-biotinylated probe, O-JH108 for *manY* or SsrA-bio for *ssrA*. Detection was performed according to BrightStar BioDetect kit (Ambion) specifications.

5′ RACE

5′ RACE was performed as described previously (26) using the *manY*-specific primer O-JH139 with RNA isolated from DJ480 cells grown to an OD$_{600}$ ∼0.5 in minimal MOPS + 0.2% Mannose.

SgrS random mutagenesis

The *sgrS* region of P$_{lac}$-*sgrS* (pLCV1) was mutated using the GeneMorph EZclone II kit (Stratagene) and the resulting mutated plasmid library transformed into a

manX′–′lacZ, Δ*sgrS*, *lacI*$^{q+}$ strain (JH116). Mutant plasmids that were unable to regulate *manX′–′lacZ* activity were isolated and transformed into a *ptsG′–′lacZ*, Δ*sgrS*, *lacI*$^{q+}$ strain (JH171). Plasmids that were able to negatively regulate *ptsG′–′lacZ* activity were sequenced.

In vitro RNA footprinting

In vitro transcription templates were generated by PCR using gene-specific oligonucleotides containing the T7 promoter sequence. Oligos O-JH218/O-JH169 were used to generate a *manX* template (from −115 to +102 relative to the translational start site), oligos O-JH236/O-JH241 were used to generate a *ptsG* template (from −103 to +104 relative to the translational start site) and oligos O-JH219/O-JH119 were used to generate an *sgrS* template. *In vitro* transcription was performed with the PCR templates using the MEGAscript T7 Kit (Ambion). The resulting RNA was 5′-end labeled using the KinaseMax Kit (Ambion). Footprinting reactions were performed as described previously (5) with the following changes. Ten picomol of unlabeled SgrS, *manX* mRNA or *ptsG* mRNA was incubated with 0.1 pmol of 5′-end labeled *manX* mRNA, *ptsG* mRNA or SgrS at 37°C for 15 min in 1× Structure Buffer (Ambion) in the presence or absence of 300 nM Hfq.

RNA Structure Analysis

RNA structure was analyzed using the RNA folding program Mfold (27). Structures with the lowest Δ*G* that were most consistent with experimental data from footprinting experiments (if available) are shown.

RESULTS

manXYZ is post-transcriptionally regulated by SgrS

Preliminary microarray results suggested that *manXYZ* mRNA is negatively regulated by SgrS (our unpublished data). In order to investigate whether regulation of the polycistronic *manXYZ* mRNA by SgrS was direct, a translational *manX′–′lacZ* fusion was created at the *manX* locus. A synthetic constitutive promoter, Cp19 (28), was used to drive transcription of the *manX′–′lacZ* fusion in order eliminate indirect effects due to transcriptional regulation (Figure 1A). β-Galactosidase activities of wild-type and Δ*sgrS* mutant cells harboring the fusions were monitored after stress was induced by addition of αMG to cultures. Wild-type cells had ∼65% lower *manX′–′lacZ* fusion activity than Δ*sgrS* cells (Figure 1B). These data indicate that *manX* is post-transcriptionally regulated in an SgrS-dependent manner under glucose–phosphate stress conditions.

To determine whether SgrS could regulate *manX* in the absence of other stress-inducible factors, a P$_{lac}$-*sgrS* plasmid and an empty vector control were transformed into an *sgrS* mutant host containing the same reporter constructs shown in Figure 1A. Regulation of *manX* translation in cells containing P$_{lac}$-*sgrS* was similar to that in cells where chromosomal *sgrS* expression was induced by αMG. Expression of the fusion was reduced upon *sgrS* induction by 75% (Figure 1C). These results suggest that SgrS is sufficient to regulate *manX* translation in the absence of other stress-inducible factors. In order to compare SgrS regulation of *manX* and *ptsG*, a Cp19-*ptsG′–′lacZ* fusion was also analyzed for regulation by P$_{lac}$-*sgrS*. The *ptsG′–′lacZ* fusion activity responded similarly to the *manX′–′lacZ* fusion; upon *sgrS* induction, it was downregulated by ∼75% (Figure 1C). Since *ptsG*
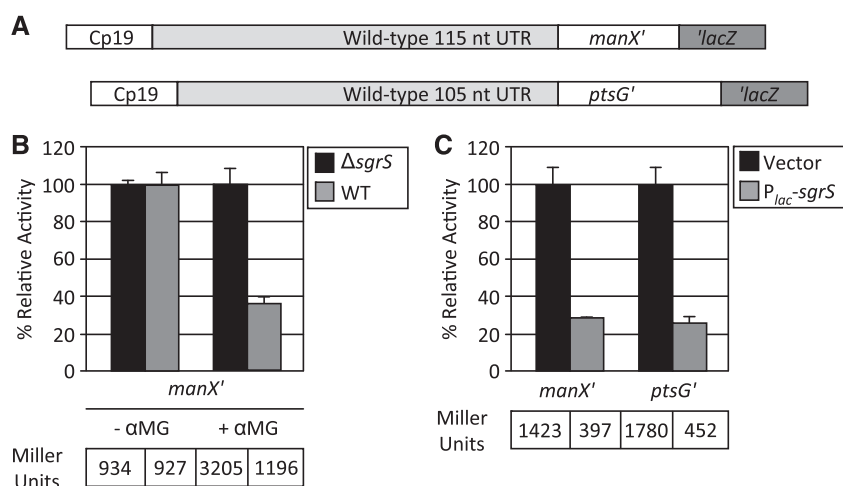

Figure 1. *manX* translation is repressed in an SgrS-dependent manner. (**A**) Chromosomal *lacZ* translational fusions were constructed at the native loci. The native promoters of *ptsG* and *manX* were replaced with the constitutive Cp19 promoter (28). (**B**) Cp19-*manX′–′lacZ* strains in Δ*sgrS* (JH143) or *sgrS*$^{+}$ (wild-type, JH138) backgrounds were grown to early log phase and 0.5% αMG was added. Samples were harvested 60 min after αMG addition and assayed for β-galactosidase activity. Specific activities in all samples were normalized to the levels in the Δ*sgrS* strain to yield percentage relative activity (reported in the graph). Specific activity values in Miller units are reported below the graph. (**C**) Strains with Cp19-*manX′–′lacZ* (JH193) or Cp19-*ptsG′–′lacZ* (JH184) carrying an empty vector or P$_{lac}$-*sgrS* were grown to early log phase and 0.1 mM IPTG was added. Samples were harvested 60 min after IPTG addition and assayed for β-galactosidase activity. Specific activities were normalized and data reported as in part (B).

mRNA is an established target of SgrS (9,11), this finding lends further weight to the hypothesis that SgrS directly regulates *manXYZ*. Because *manX'–'lacZ* is regulated by SgrS in the absence of the downstream *manY* and *manZ* sequences, we hypothesized that base pairing between SgrS and the *manXYZ* transcript involves the *manX* translation initiation region.

A *manX'–'lacZ* fusion under control of the native *manX* promoter was also tested for regulation by SgrS induced under stress conditions or from a plasmid. In all cases, the results were analogous to those for the Cp19-controlled fusions (data not shown).

SgrS stimulates degradation of *manXYZ* mRNA

To assess whether SgrS-dependent regulation of *manX* translation affected *manXYZ* mRNA stability, northern blots were performed on RNA samples from wild-type and Δ*sgrS* strains carrying Cp19-*manXYZ* constructs (Figure 2A). A *manX*-specific probe hybridized to a ~2.8 kb band corresponding to the full-length *manXYZ* mRNA (data not shown). A *manY*-specific probe hybridized to the ~2.8 kb band as well as an additional ~1.8 kb band (Figure 2B). When RNA from a Δ*manXYZ*

Figure 2. *manXYZ* mRNA is destabilized in an SgrS-dependent manner and *manYZ* mRNA is processed in an SgrS-independent manner. (**A**) The Cp19 constitutive promoter replaced the *manXYZ* promoter at the native locus. (**B**) Cp19-*manXYZ* in wild-type *sgrS$^+$* (JH124) or Δ*sgrS* (JH125) backgrounds were grown to mid-log phase and 0.5% αMG was added to the cultures. RNA was extracted at times indicated and analyzed by northern Blot using *manY*- or *ssrA*-specific probes. SsrA served as the loading control. ImageJ was used to quantify band intensities and correct for uneven loading. Corrected intensities for each band were then normalized to time 0 (set at 1.0). Expression relative to time zero is reported below the blot ('Rel. Exp.'). (**C**) 5′ RACE analysis of *manY* was performed on RNA extracted from wild-type (DJ480) cells grown to mid-log phase. The sequences of *manY* 5′-ends and the frequency of their occurrence in sequenced clones (out of eight total) are shown. The *manY* start codon is underlined.

strain was probed with the *manY*-specific probe, neither of these bands was present (data not shown). The 1.8 kb band is the size predicted for a *manYZ* transcript. 5′ RACE analysis (26) was utilized to distinguish whether *manYZ* was a newly initiated transcript or a processed product. This analysis revealed that the *manYZ* mRNA contained a monophosphate end, indicative of a processed transcript (Supplementary Figure S1). Furthermore, several different 5′-ends of the *manYZ* species mapped to a region between *manX* and *manY* that was AU-rich (Figure 2C). These sequences resemble RNase E recognition and cleavage sites (29–31). A transcriptional *manY'–lacZ* fusion confirmed that there is no promoter activity associated with the *manX–manY* intergenic region (data not shown). All together, these data suggested that *manYZ* is processed from *manXYZ*.

We proceeded by examining SgrS regulation of both *manXYZ* and *manYZ* mRNA levels. In wild-type cells, a decrease in the levels of the *manXYZ* transcript was apparent following αMG addition, while levels of the *manYZ* mRNA remained relatively steady (Figure 2B, lanes 1–5). In contrast, cells lacking *sgrS* displayed greatly increased levels of *manXYZ* transcript and relatively constant levels of *manYZ* transcript after αMG addition (Figure 2B, lanes 6–10). Because the transcription of *manXYZ* in this experiment is driven by the constitutive Cp19 promoter (28), we hypothesize that changes in steady-state levels of *manXYZ* mRNA reflect changes in stability rather than rates of synthesis. Therefore, these results suggest that SgrS is responsible for decreasing the stability of the full-length *manXYZ* transcript but has no significant effect on the stability of the *manYZ* transcript.

To test whether the apparent accumulation of *manXYZ* mRNA in *sgrS* mutant cells (Figure 2B, lanes 6–10) reflected a *manXYZ*-specific post-transcriptional mechanism of regulation, we examined levels of the *ptsG* mRNA expressed from the Cp19 promoter in *sgrS$^+$* and *sgrS* mutant cells exposed to αMG. This experiment showed that *ptsG* mRNA does not accumulate in the *sgrS* mutant strain after αMG addition (data not shown), in contrast to the *manXYZ* mRNA. We also examined *manXYZ* and *manYZ* mRNAs (expressed from the Cp19 promoter) in Δ*sgrS* cells in the absence of αMG and found no accumulation over time in non-stressed cells (data not shown). Together, these data suggest that the accumulation of *manXYZ* mRNA in *sgrS* mutant cells reflects a post-transcriptional mechanism of regulation that is stress dependent.

Biochemical demonstration of SgrS base pairing with target mRNAs

SgrS regulates the *ptsG* mRNA by a base pairing mechanism involving the region surrounding the *ptsG* ribosome binding site. In order to narrow down the region of *manX* required for regulation by SgrS, the 115 nt 5′ UTR of the *manX'–'lacZ* fusion was truncated by moving the Cp19 promoter closer to the *manX* translational start site. A fusion containing 30 nt upstream of the *manX* start codon was constructed (denoted as *manX$_{30}$'–'lacZ*)
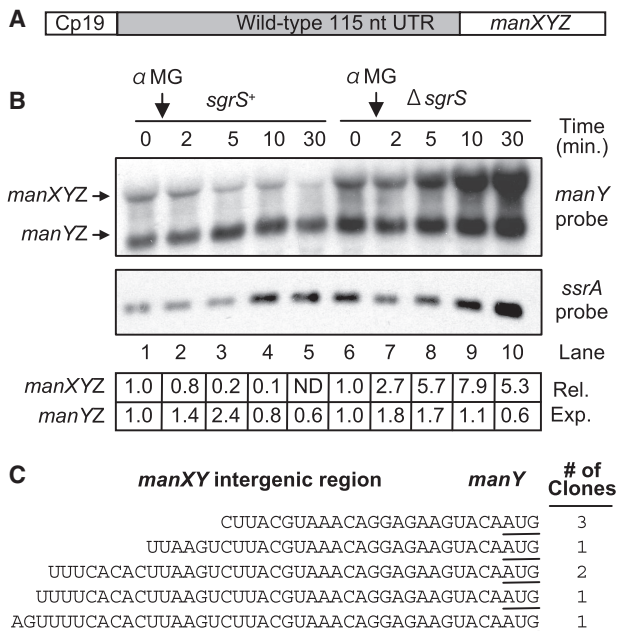
(Supplementary Figure S2A). Activity of the $manX_{30}'$–$'lacZ$ fusion was monitored in the presence or absence of ectopically expressed $sgrS$. Cells showed a pattern of regulation by SgrS that was similar to the regulation of the full-length Cp19-$manX'$–$'lacZ$ fusion, i.e. a 65% decrease in β-galactosidase activity when SgrS was present (Supplementary Figure S2B). Truncating the 5′-UTR further (to 20 nt) resulted in an unstable $manXYZ$

transcript regardless of the presence or absence of SgrS (data not shown). Therefore it was concluded that at most, 30 nt of the $manX$ 5′-UTR and 102 nt of $manX$ coding sequence are needed for regulation by SgrS.

Given that the region contained in the $manX_{30}'$–$'lacZ$ fusion is sufficient for regulation by SgrS, potential base pairing interactions between SgrS and the $manX$ sequences contained in this region were examined. A region of
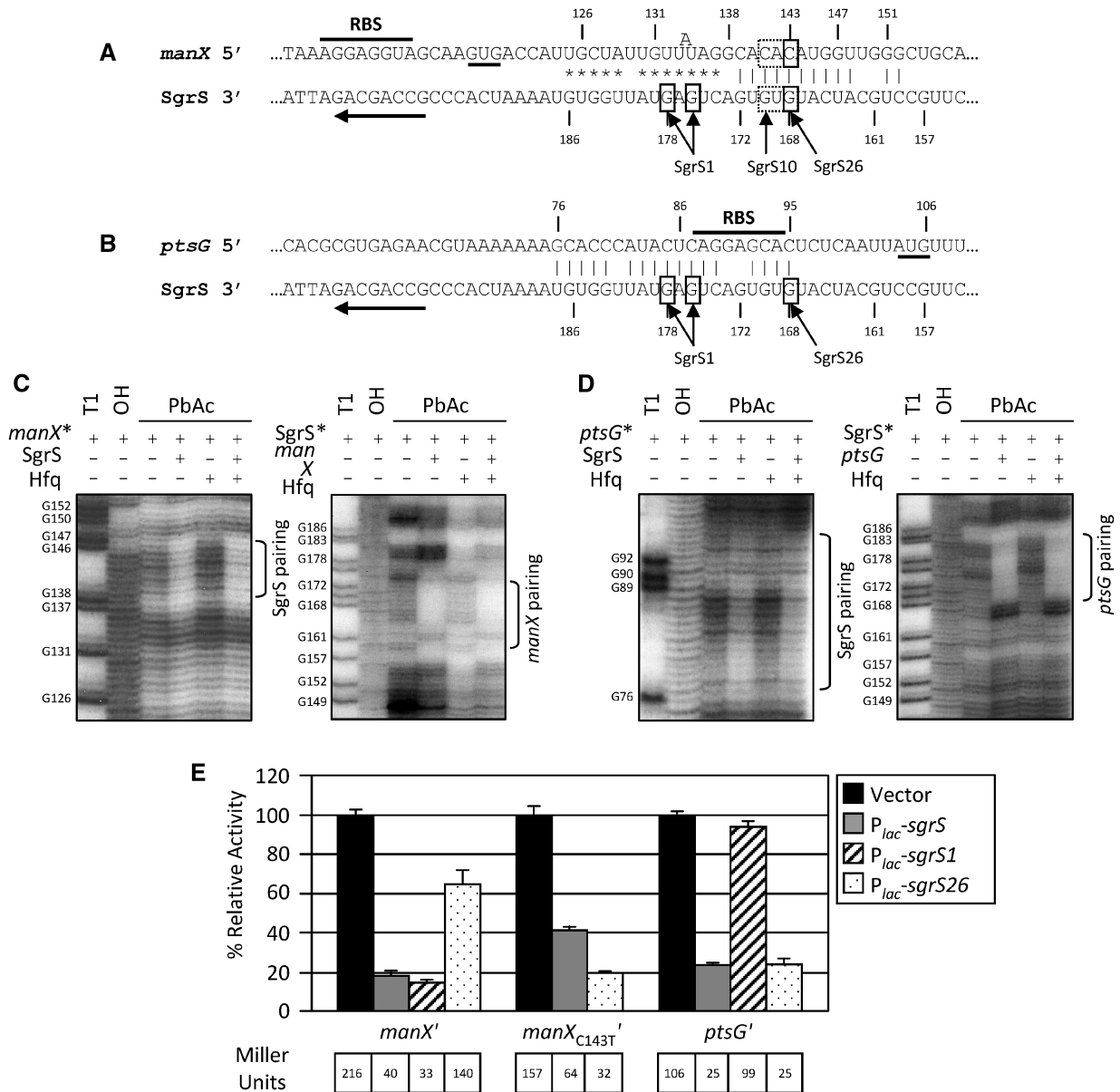

Figure 3. SgrS base pairing with mRNA targets. (**A**) Predicted base pairing between $manX$ mRNA and SgrS. Pairing confirmed by footprinting and genetic analyses is indicated by vertical lines and pairing predicted but not experimentally supported is indicated by asterisks. The $manX$ RBS is denoted by a line above the sequence; the $manX$ start codon is underlined; half of the inverted repeat of the SgrS terminator is denoted by the long arrow below the sequence. The boxed bases were mutated to test base pairing. Arrows and allele names (SgrS1, SgrS26 and SgrS10) indicate positions of mutations in different SgrS mutants (also see Supplementary Table S1). (**B**) Base pairing between SgrS and $ptsG$ mRNA. See part (A) for further description. (**C**) *In vitro* transcribed $manX$ mRNA containing the entire $manX$ sequence present in the $manX'$–$'lacZ$ fusion was end-labeled with [32]P ($manX^*$) and incubated with unlabeled SgrS where noted and treated with: T1, RNase T1; OH, alkaline hydrolysis; PbAc, lead acetate. The positions of G residues are shown. *In vitro* transcribed SgrS was labeled with [32]P (SgrS*) and incubated with unlabeled $manX$ where noted. (**D**) Interactions between SgrS and $ptsG$ mRNA were mapped as described in part (C). Abbreviations are as described in part (C). (**E**) $manX'$–$'lacZ$ (JH116), $manX_{C143T}'$–$'lacZ$ (JH216) and $ptsG'$–$'lacZ$ (JH171) strains carrying an empty vector, P_{lac}-$sgrS$, P_{lac}-$sgrS1$ or P_{lac}-$sgrS26$ were analyzed for β-galactosidase activity as described in Figure 1C.

complementarity between the 3′ region of SgrS and the coding region of *manX* was identified (Figure 3A). To test the base pairing prediction, footprinting analyses were performed with *in vitro*-transcribed SgrS and *manX* RNAs. Experiments using labeled *manX* mRNA revealed SgrS-dependent protection of *manX* bases from C139 to G147 (Figure 3C). This region corresponds to the longest contiguous stretch of predicted base pairing located from 23 to 33 nt downstream of the *manX* translational start (Figure 3A). The reverse analysis was done with labeled SgrS to determine the region that interacts with *manX* mRNA. The region of SgrS predicted to base pair with *manX* (from C159 to A180, Figure 3A) was mostly single stranded in the absence of target mRNA (Figure 3C), while a footprint spanning SgrS bases from A163 to G172 was observed in the presence of *manX* mRNA (Figure 3C). This result was consistent with interactions in the longest contiguous stretch of base pairing indicated in Figure 3A.

The sequences in SgrS that base pair with *manX* in footprinting experiments partially overlap with sequences predicted to pair with *ptsG* mRNA (Figure 3A and B). Several studies (11,15) have genetically demonstrated the importance of interactions between SgrS and *ptsG* mRNA that encompass residues from C174 to U181 of SgrS and from A82 to G89 of *ptsG* mRNA (Figure 3B). In particular, mutations in residues G176 and G178 of SgrS effectively destroy regulation of *ptsG* mRNA, while compensatory mutations in *ptsG* restore regulation (11). Additional complementarity on either side of this 'core' SgrS-*ptsG* mRNA interaction is predicted, but interactions have not been verified either genetically or biochemically. Therefore, footprinting experiments were carried out to map SgrS binding sites on *ptsG* mRNA and *vice versa*. These experiments showed a clear SgrS footprint on *ptsG* mRNA spanning residues from A82 to G89 (Figure 3D), which is consistent with the core interaction region demonstrated genetically. There was also weak protection of *ptsG* mRNA residues from G76 to A78 (upstream of the core region) and from C92 to C95 (downstream of the core region). A *ptsG* mRNA footprint on SgrS showed protection of SgrS bases from G168 to U181 (Figure 3D), consistent with interactions in the core region and downstream (with respect to the *ptsG* mRNA). Together, the footprinting experiments demonstrated two important things: (i) different residues of SgrS are involved in specific base pairing interactions with different targets and (ii) base pairing involves different regions of different targets, i.e. overlapping the ribosome binding site of *ptsG* and within the coding sequence of *manX*.

Genetic demonstration of SGRS Base pairing with *manX* mRNA

As a second confirmation of SgrS–*manX* mRNA interactions, a genetic approach utilizing random mutagenesis of SgrS was performed. A screen was conducted to identify SgrS mutants that failed to regulate *manX′–′lacZ* but retained regulation of *ptsG′–′lacZ*. These criteria were used in order to avoid isolating mutations that had non-specific deleterious effects on SgrS structure

and function. Numerous mutations were found that impaired regulation of both fusions, but mutations in only two residues, T169 and G170, had a specific phenotype for regulation of *manX′–′lacZ* (data not shown); these residues are encompassed within the region protected in footprinting experiments (Figure 3).

To further genetically test the base pairing interactions between SgrS and *manX* mRNA, wild-type and mutant alleles of SgrS were tested for regulation of wild-type and compensatory mutant *manX′–′lacZ* fusions as well as a wild-type *ptsG′–′lacZ* fusion (Figure 3E). Mutant SgrS alleles contained either G176C, G178C (*sgrS1*), which should interfere with regulation of *ptsG* (15) or G168A (*sgrS26*), which should interfere with regulation of *manX*. The predicted structures of both SgrS mutants were identical to that of wild-type SgrS [according to Mfold (27), data not shown]. Wild-type SgrS and SgrS1 (G176C, G178C) regulated *manX′–′lacZ* to the same extent (~80% repression), while SgrS26 (G168A) was defective in regulating *manX′–′lacZ* (~35% repression) (Figure 3E, left panel). The results for regulation of wild-type *ptsG′–′lacZ* by each of these mutants were the opposite; wild-type SgrS and SgrS26 regulated *ptsG′–′lacZ* to the same extent (~80% repression), whereas SgrS1 completely lost the ability to repress (Figure 3E, right panel). These results strongly suggest that each of these mutants retains the appropriate structure and that loss of regulation reflects disruption of target-specific base pairing interactions. To further confirm direct base pairing between SgrS and *manX* mRNA, a compensatory mutation in *manX* (C143T), which should restore pairing with SgrS26 and disrupt pairing with wild-type SgrS was constructed in the context of the reporter fusion (designated *manX*$_{C143T}$*′–′lacZ*). Consistent with this prediction, wild-type SgrS was deficient in regulating *manX*$_{C143T}$*′–′lacZ* (~60% repression) whereas SgrS26 gave full 80% repression (Figure 3E, center panel).

It is worth noting that the footprinting experiments accurately report relevant *in vivo* base pairing interactions. Protection of SgrS residues 174–186 and *manX* mRNA residues 125–137 was not observed (Figure 3C), despite the complementarity in this region (Figure 3A) and the apparently single-stranded conformation *in vitro* (based on susceptibility to cleavage by lead acetate, Figure 3C). Consistent with this, mutations in SgrS (in the *sgrS1* allele) that would disrupt the base pairing of this region (complementarity denoted by asterisks, Figure 3A) had no effect on the regulation *in vivo*. Similarly, for SgrS:*ptsG* mRNA interactions, the most strongly protected residues *in vitro* (SgrS residues 174–181 and *ptsG* mRNA residues 82–89) were the most relevant for *in vivo* regulation (Figure 3B, D and E).

The structure of SgrS alone (Fig. 3C, D, left panels) corresponded very well to the Mfold (27) prediction (Figure 4B). The SgrS bases that participate in pairing with *manX* mRNA are mostly single stranded, with the exception of three residues that participate in formation of a short stem (residues 163–165, Figures 3C and 4B). Residues 159 and 160 are located in a small bubble in SgrS alone; in the presence of *manX* mRNA residues 159–160 and 163–172 are protected and residues 161 and
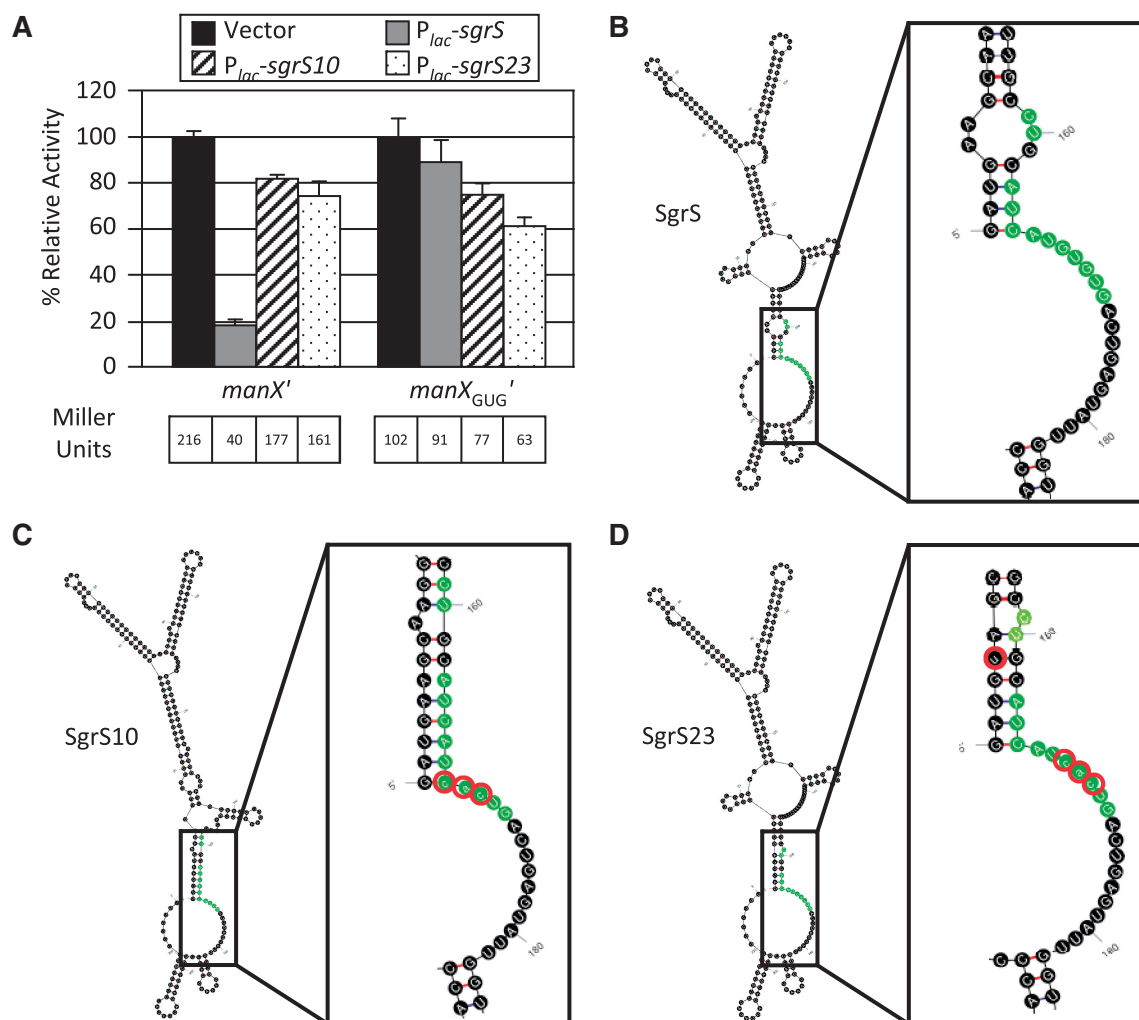
Figure 4. Structural changes in SgrS mutants. (**A**) *manX'–'lacZ* (JH116) and *manX*~GUG~'*–'lacZ* (JH229) strains carrying an empty vector, P~lac~-*sgrS*, P~lac~-*sgrS10* or P~lac~-*sgrS23* were analyzed for β-galactosidase activity as described in Figure 1C. (**B**) Mfold prediction of wild-type SgrS structure, which is consistent with footprinting of SgrS alone (Figure 3C). (**C**) Mfold prediction of SgrS10 structure. Strong base pairing interactions are indicated by a red line. Mutated bases are circled in red. (**D**) Mfold prediction of SgrS23 structure. Strong base pairing interactions are indicated by a red line. Mutated bases are circled in red.

162 become hypersensitive (Figure 3C). In the course of testing certain SgrS and *manX* mutant pairs, we observed that mutation of some SgrS residues resulted in significant predicted structural changes in SgrS in the region that interacts with *manX* mRNA. For example, mutation of SgrS residues 168–170 from GUG to CAC (in allele *sgrS10*, Figure 3A, Supplementary Table S1) not only disrupted complementarity with wild-type *manX*, but also resulted in sequestration of the majority of the *manX* mRNA pairing region of SgrS in a stem (compare the wild-type SgrS structure, Figure 4B, to the mutant structure, Figure 4C). This sequestration could be partially alleviated by making an additional mutation in SgrS (A5U, allele *sgrS23*, Fig. 4D). To determine how these changes would affect regulation of *manX*, we assayed the activity of these mutants in wild-type *manX'–'lacZ* and mutant *manX*~GUG~'*–'lacZ* strains (the latter fusion contains mutations that would restore complementarity with the SgrS mutant alleles). As predicted, wild-type

SgrS repressed wild-type *manX'–'lacZ* and both mutant alleles (SgrS10 and SgrS23) were strongly impaired for regulation (Figure 4A, left panel). In the *manX*~GUG~'*–'lacZ* background, wild-type SgrS lost the ability to regulate, again consistent with the involvement of these residues in SgrS:*manX* mRNA base pairing interactions (Figure 4B, right panel). SgrS10 regulated *manX*~GUG~'*–'lacZ* only slightly better than wild-type SgrS, despite having the compensatory changes that should have restored base pairing. This was consistent with the predicted sequestration of most of the base pairing region (Figure 4C). The additional mutation in SgrS23 gave a slight improvement in the regulation of *manX*~GUG~'*–'lacZ* compared to the wild-type and SgrS10 alleles, but full repression was not restored, likely because the structure of SgrS23 is still altered compared to wild-type SgrS (compare Figure 4B and D). Northern blots showed that SgrS10 and SgrS23 were produced at levels similar to wild-type SgrS and both of these mutants retained

regulation of *ptsG'–'lacZ* (data not shown), which was not surprising since the residues in SgrS important for interaction with *ptsG* mRNA remained unpaired in the mutant structures (see residues from 174 to 181 in Figure 4C and D). Failure of compensatory mutations to fully restore wild-type levels of regulation has been observed for other sRNA:mRNA pairs (5,32,33) and has been interpreted to mean that both sequence and structure of the two RNAs are important for their interactions and that the structures of one or both molecules are altered by certain mutations. These results are certainly consistent with that explanation.

Degradation of *manXYZ* is not required for SgrS regulation of *manX* translation

Although SgrS promotes degradation of the *ptsG* message, this is not required for translational regulation (11). SgrS-mediated translational repression of *ptsG* is thought to occur through a ribosome occlusion mechanism, since residues of the *ptsG* Shine-Dalgarno sequence are involved in base pairing interactions with SgrS (9,11). Given that SgrS base pairs downstream of the *manX* ATG and we showed that the *manXYZ* mRNA is degraded when SgrS is expressed, we wanted to determine if SgrS-mediated translational repression of *manX* requires degradation of the *manXYZ* mRNA. For that reason, activities of *manX* and *ptsG* translational fusions were compared in wild-type and *rne131* backgrounds in the presence or absence of *sgrS*. The *E. coli rne131* allele encodes a C-terminally truncated RNase E that does not associate with Hfq or degradosome proteins. C-terminal RNase E mutants have been shown to be defective for degrading other sRNA–mRNA complexes, including SgrS-*ptsG* mRNA (34–36). In accordance with previous findings (36), the *rne131* allele did not affect the ability of SgrS to repress translation of *ptsG'–'lacZ* (Figure 5A). Similar results were observed with *manX'–'lacZ* (Figure 5A) suggesting that like *ptsG*, *manX* regulation by SgrS does not require degradosome-mediated mRNA degradation.

To confirm that SgrS-mediated degradation of *manXYZ* mRNA was abolished in the *rne131* background, Northern blot analysis was performed on *sgrS*⁺ and Δ*sgrS* cells in wild-type and *rne131* strains. As expected, *manXYZ* levels decreased in *sgrS*⁺ cells upon αMG addition (Figure 5B, lanes 1–3) but accumulated in Δ*sgrS* cells (Figure 5B, lanes 4–6). In contrast, *sgrS*⁺ and Δ*sgrS* cells both had increased levels of *manXYZ* mRNA following αMG addition in the *rne131* background (Figure 5B, lanes 7–12), confirming that degradation was abolished in these strains. Interestingly, the *manYZ* transcript was present at much lower levels in the *rne131* strains (Figure 5B, lanes 7–12), suggesting that *manYZ* processing involves RNase E. Combined with the results from translational fusions in the *rne131* background (Figure 5A), these data are consistent with the hypothesis that *manX* regulation by SgrS occurs primarily at the level of translational inhibition, rather than mRNA degradation.
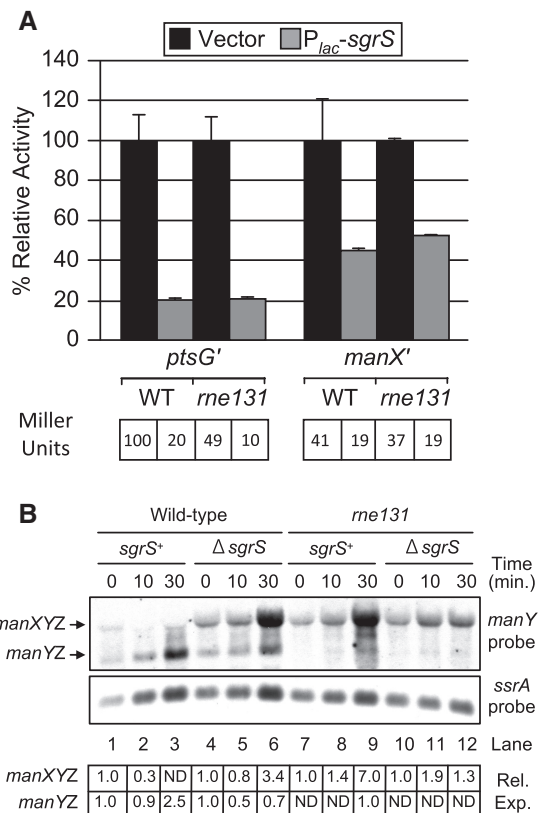

Figure 5. SgrS-dependent *manX* regulation does not require the degradosome. (**A**) *ptsG'–'lacZ* strains carrying an empty vector or P*lac*-*sgrS* were analyzed in a wild-type (JH258) or *rne131* (JH248) background and compared to *manX'–'lacZ* strains carrying an empty vector or P*lac*-*sgrS* in wild-type (JH255) or *rne131* (JH246) backgrounds. β-galactosidase assays were performed as described in Figure 1C. (**B**) *manXYZ* mRNA from *sgrS*⁺ (DJ480) or Δ*sgrS* (CV100) backgrounds were compared to *manXYZ* mRNA from *rne131* strains containing wild-type *sgrS* (EM1377) or the *sgrS* deletion (JH273). RNA was harvested when cells reached mid-log phase (time 0) and at times indicated following addition of 0.5% alpha-MG. RNA was analyzed by Northern blotting as described in Figure 2B. ImageJ was used to quantify band intensities and correct for uneven loading. Corrected intensities for each band were then normalized to time zero (set at 1.0). Expression relative to time zero is reported below the blot.

The weak start codon of *manX* does not influence SgrS regulation

Work by Kawamoto *et al.* (36) suggested that co-translational membrane localization of *ptsG* mRNA is required for *ptsG* regulation by SgrS. The data support a model whereby *ptsG* mRNA membrane localization decreases translational efficiency of the *ptsG* message, thus allowing SgrS to compete effectively with ribosomes for binding to the translation initiation region of the *ptsG* mRNA. Since *manX* encodes the cytoplasmic component of the transporter, the *manX'–'lacZ* transcript would not be localized to the membrane, therefore this cannot be a contributing factor to regulation by SgrS. We did notice, however, that *manX* has a conserved GTG start codon (Figure 7B), which promotes decreased rates of translation initiation compared with ATG start codons (37). We therefore tested the hypothesis that the weaker start codon might be important for SgrS

regulation of *manX*. A GTG to ATG mutation was made in the context of the *manX′–′lacZ* chromosomal fusion. Though the ATG mutation did increase basal levels of *manX′–′lacZ* translation as expected, it did not alter the fold-repression when SgrS was induced from the chromosome (Supplementary Figure S3A) or a plasmid (Supplementary Figure S3B), indicating that the weaker start codon is not required for regulation by SgrS.

ManXYZ proteins transport stress-inducing sugar analogs

It is well established that EIICB^{Glc} (PtsG) is involved in generating glucose–phosphate stress because it transports and phosphorylates sugars or sugar analogs like αMG that accumulate under certain conditions. SgrS relieves the stress by regulating *ptsG* mRNA, preventing synthesis of new EIICB^{Glc} and therefore decreasing accumulation of sugar–phosphates (8–10,38). We hypothesized that *manXYZ* also contributes to glucose–phosphate stress since it transports glucose and αMG and is regulated by SgrS. Another glucose analog, 2-deoxyglucose (2DG) is a good substrate for the EII^{Man} system (ManXYZ) but only weakly transported by EIICB^{Glc} (39–43); upon transport, 2DG becomes 2-deoxyglucose-6-phosphate (2DG6P). It was previously shown that high levels of 2DG6P cause growth inhibition in *E. coli* cells (44), however, we had not tested whether 2DG6P induces the SgrS-mediated stress response. To test the role of *manXYZ* in stress caused by these two glucose analogs, strains were constructed with mutations in *ptsG* and *manXYZ* individually and in combination. Induction of the stress response was monitored using a chromosomal P$_{sgrS}$–*lacZ* reporter. The reporter fusion was not induced in the absence of sugar analogs (Figure 6A and B, left panels), as expected. When wild-type cells were exposed to 0.1% αMG, P$_{sgrS}$–*lacZ* activity was induced by 126-fold over –αMG levels (see Miller Units, Figure 6A), indicating that the stress response was induced. The reporter was still induced slightly in the ΔptsG strain in the presence of αMG, albeit to a lower level (21.5-fold compared to uninduced), suggesting that cells take up sufficient αMG by an EIICB^{Glc}-independent route to slightly induce the stress response. In the ΔptsG, ΔmanXYZ double mutant the reporter was not activated in the presence of αMG, indicating that in the absence of EIICB^{Glc}, the EII^{Man} system is responsible for transporting the αMG that induces the stress response.

In the presence of 0.1% 2DG, the P$_{sgrS}$–*lacZ* fusion was activated in wild-type cells by 36-fold compared to uninduced levels (see Miller Units, Figure 6B). This indicated that 2DG does induce the glucose–phosphate stress response. In the ΔptsG background, induction of the reporter was similar to the induction in the wild-type strain, implying that EIICB^{Glc} does not contribute significantly to *sgrS* induction in response to 2DG. In contrast, in the ΔmanXYZ strain, the P$_{sgrS}$–*lacZ* reporter was induced only 1.7-fold (Figure 6B). The reporter was also induced by 1.7-fold in the ΔptsG ΔmanXYZ double mutant. These results suggest that EII^{Man} is almost fully responsible for transporting 2DG, which induces the stress response. Cumulatively, these findings suggest that
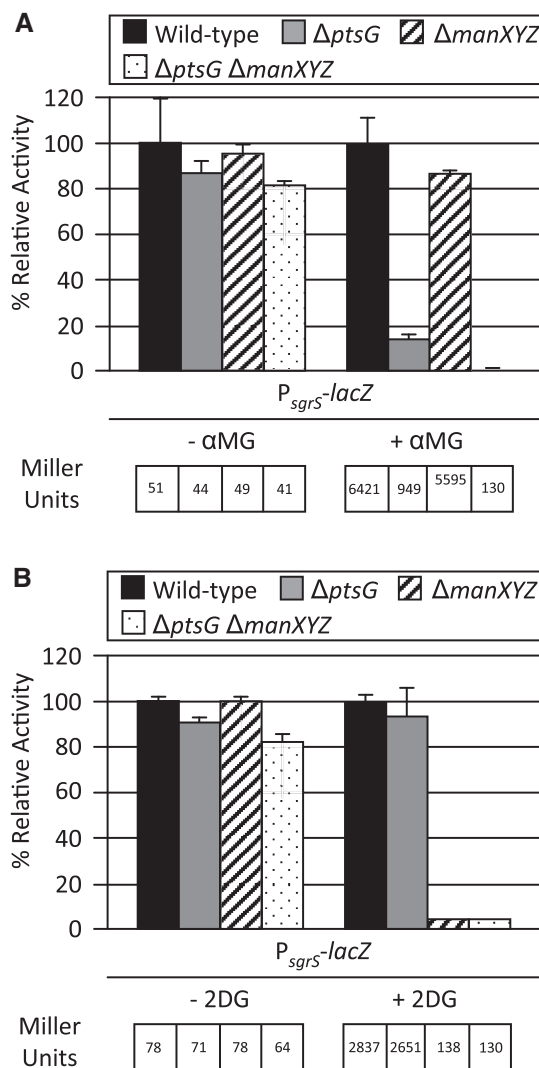

Figure 6. Glucose–phosphate stress is induced by sugar analogs transported by EIICB^{Glc} and EII^{Man}. Wild-type (BAH100), ΔptsG (CS177), ΔmanXYZ (CS178) or ΔptsG ΔmanXYZ (CS179) strains carrying the P$_{sgrS}$–*lacZ* reporter were grown to early log phase at which time 0.1% αMG (**A**) or 0.1% 2DG (**B**) was added. Samples were harvested 120 min after αMG/2DG addition and assayed for β-galactosidase activity. Miller units from all samples were normalized to the wild-type levels to yield relative relative activity. Specific activity values (Miller units) are reported below each graph.

SgrS-mediated regulation of *manXYZ* is physiologically relevant for minimizing the stress caused by accumulation of non-metabolizable sugar–phosphates.

The SgrS regulon does not appear to be fully conserved among different organisms

Two recent studies from our laboratory (15,45) suggested that regulation of *ptsG* by SgrS is conserved among enterobacterial species that possess SgrS orthologs. We investigated whether this was also true for SgrS translational regulation of *manX*. SgrS orthologs from *Salmonella typhimurium*, *Klebsiella pneumoniae*, *E. carotovora* and *Y. pestis* regulate *E. coli ptsG*
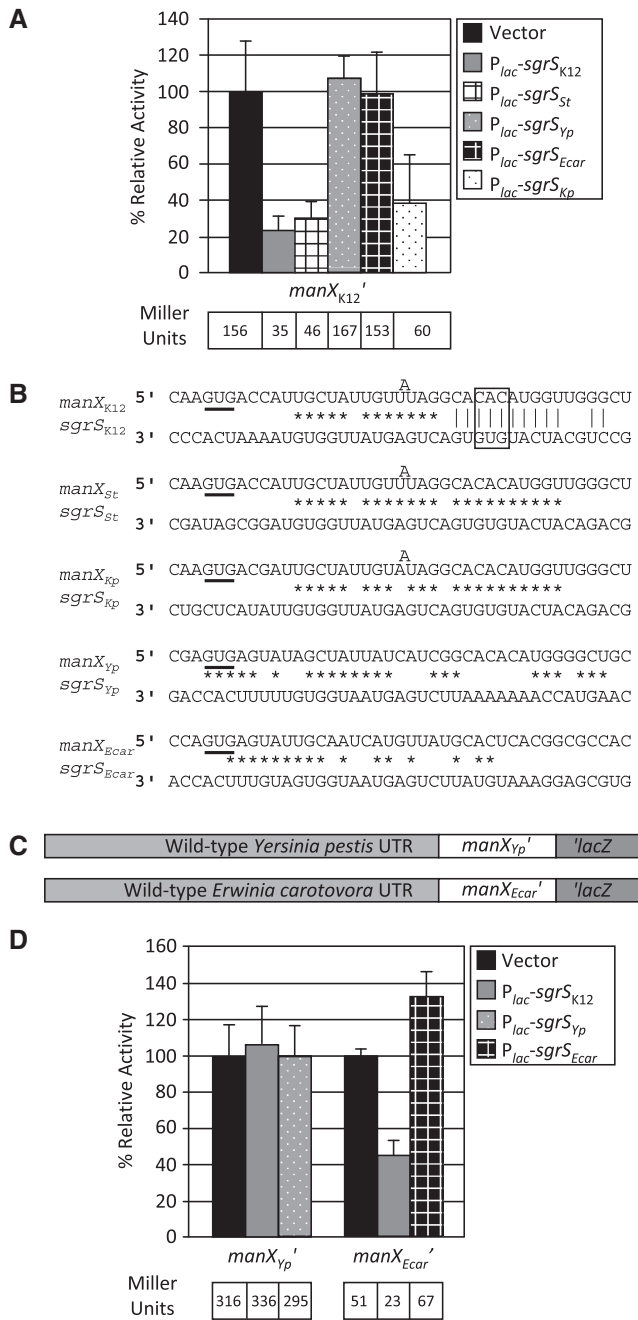
A

(Bar graph: % Relative Activity, y-axis 0–140, for manX_K12′)

Legend:
- Vector
- P_lac-sgrS_K12
- P_lac-sgrS_St
- P_lac-sgrS_Yp
- P_lac-sgrS_Ecar
- P_lac-sgrS_Kp

Miller Units	156	35	46	167	153	60

B

```
          A
manX_K12 5' CAAGUGACCAUUGCUAUUGUUUAGGCA CAC AUGGUUGGGCU
sgrS_K12 3' CCCACUAAAAUGUGGUUAUGAGUCAGU GUG UACUACGUCCG
              *****  *******  |||||||||||   ||

          A
manX_St  5' CAAGUGACCAUUGCUAUUGUUUAGGCACACAUGGUUGGGCU
sgrS_St  3' CGAUAGCGGAUGUGGUUAUGAGUCAGUGUGUACUACAGACG
              *****  *******  **********

          A
manX_Kp  5' CAAGUGACGAUUGCUAUUGUAUAGGCACACAUGGUUGGGCU
sgrS_Kp  3' CUGCUCAUAUUGUGGUUAUGAGUCAGUGUGUACUACAGACG
              *****  ***  ***  **********

manX_Yp  5' CGAGUGAGUAUAGCUAUUAUCAUCGGCACACAUGGGGCUGC
sgrS_Yp  3' GACCACUUUUUGUGGUUAUGAGUCUUAAAAAAAACCAUGAAC
             *****  *  ********   ***     ***  ***

manX_Ecar5' CCAGUGAGUAUUGCAAUCAUGUUAUGCACUCACGGCGCCAC
sgrS_Ecar3' ACCACUUUGUAGUGGUUAUGAGUCUUAUGUAAAGGAGCGUG
             *********  *   **  *     *  **
```

C

| Wild-type *Yersinia pestis* UTR | manX_Yp′ | ′lacZ |

| Wild-type *Erwinia carotovora* UTR | manX_Ecar′ | ′lacZ |

D

(Bar graph: % Relative Activity, y-axis 0–160, for manX_Yp′ and manX_Ecar′)

Legend:
- Vector
- P_lac-sgrS_K12
- P_lac-sgrS_Yp
- P_lac-sgrS_Ecar

Miller Units	316	336	295		51	23	67

Figure 7. SgrS-dependent regulation of *manX* is not entirely conserved among enteric species. (**A**) The *E. coli manX′–′lacZ* strain (JH116) carrying different SgrS orthologs was analyzed for β-galactosidase activity as described in Figure 1C. Abbreviations: K12, *Escherichia coli* K12; St, *Salmonella typhimurium*; Yp, *Yersinia pestis*; Ecar, *Erwinia carotovora*; Kp, *Klebsiella pneumoniae*. (**B**) Alignments of SgrS orthologs and their cognate *manX* mRNAs highlights predicted differences in base pairing interactions. The boxed region represents bases of *E. coli manX* and *SgrS* analyzed by mutational analysis in Figure 3E. Start codons for *manX* are underlined. Experimentally verified base pairing interactions are indicated by vertical lines. Other potential base pairing interactions are indicated by asterisks. (**C**) *manX* sequences from *Y. pestis* or *E. carotovora* were swapped into the *manX_K12′–′lacZ* locus as diagramed. (**D**) *manX_Yp′–′lacZ* (JH232) and *manX_Ecar′–′lacZ* (JH264) carrying an empty vector, P_lac-sgrS_K12 or the cognate P_lac-sgrS ortholog were analyzed for β-galactosidase activity as described in Figure 1C.

translation when expressed ectopically (15). Therefore, we tested these orthologs (expressed from plasmids under the control of the P_lac promoter) for their ability to regulate *E. coli manX′–′lacZ*. Northern blots performed in a previous study (15) showed that at the concentration of inducer used here, similar levels of all SgrS orthologs are produced. *E. carotovora* and *Y. pestis* SgrS orthologs did not repress *E. coli manX* translation while *S. typhimurium* and *K. pneumoniae* orthologs did (Figure 7A). This result suggested that sequences in SgrS required for regulation of *manX* translation may not be as conserved as those involved in regulating *ptsG*.

Sequence comparisons showed that the while the complementarity in the relevant base pairing region of SgrS and *manX* is conserved for *S. typhimurium* and *K. pneumoniae* SgrS and *manX* mRNA orthologs, it is not conserved for *E. carotovora* or *Y. pestis* orthologs (Figure 7B). It remained possible, however, that *E. carotovora* and *Y. pestis* SgrS orthologs regulated their cognate *manX* transcripts through the remaining regions of complementarity (Figure 7B). To test this, *E. carotovora* and *Y. pestis manX* sequences were swapped into the *E. coli* chromosome in the context of the *manX′–′lacZ* fusion (Figure 7C). The resulting *manX_Yp′–′lacZ* and *manX_Ecar′–′lacZ* fusion activities were analyzed in the presence of empty vector, P_lac-sgrS_K12 (*E. coli* SgrS) and the cognate P_lac-sgrS constructs (Figure 7D). The *manX_Yp′–′lacZ* fusion was not regulated by either *E. coli* SgrS or by *Y. pestis* SgrS. Loss of regulation of *Y. pestis manX* by *Y. pestis* SgrS can be explained by the lack of complementarity in the region corresponding to the important *E. coli* pairing region. However, it was initially surprising that *E. coli* SgrS failed to regulate *Y. pestis manX* since the *E. coli* and *Y. pestis manX* sequences are nearly identical in the relevant base pairing region (Figure 7B). We note that the accessibility of the SgrS CU residues at positions 159 and 160 (Figure 4B–D) seemed to correlate with the ability to regulate *manX*. We hypothesize that pairing of these residues helps open up the short stem downstream (sequestering residues 162–165) to allow better pairing in the longer stretch of complementarity (residues 163–175). For *Yersinia manX* and *E. coli* SgrS, the U residue of the CU pair is not complementary, so perhaps opening of the stem and accessibility of the downstream region for pairing is impaired. The *manX_Ecar′–′lacZ* was repressed by *E. coli* SgrS, suggesting that base pairing between this heterologous pair is sufficient to yield regulation. For *Erwinia manX* and *E. coli* SgrS, the pattern of predicted pairing is different. There is additional complementarity encompassing SgrS residues downstream of the stem, so perhaps the CU residues are not needed for regulation in this case. Regardless, *manX_Ecar′–′lacZ* was not regulated by *E. carotovora* SgrS, suggesting that regulation of *manX* does not occur in *E. carotovora*. Together with the previous studies from our laboratory (15,45), these data suggest that regulation of some targets, e.g. *ptsG*, is conserved, while regulation of other targets, e.g. *manXYZ*, occurs in only a subset of organisms with SgrS orthologs.

DISCUSSION

SgrS is one of the best-studied Hfq-dependent bacterial small RNAs. Studies from our laboratory (9,11,14) and the Aiba group (11) have shown that SgrS mediates the glucose–phosphate stress response in bacterial cells by two different mechanisms: (i) base pairing-dependent translational regulation of target mRNAs encoding sugar transporters and (ii) SgrT-dependent post-translational regulation of sugar transport proteins. Prior to this study, only the *ptsG* mRNA had been confirmed as a target of SgrS. Here we have demonstrated that SgrS also post-transcriptionally regulates expression of the *manXYZ* genes, which encode the mannose and alternative glucose PTS transporter. A *manX* translational fusion (Figure 1) and footprinting experiments (Figure 3C) indicate that sequences in the *manX* coding sequence, between codons 8 and 11, are involved in SgrS–*manXYZ* mRNA base pairing interactions that lead to translational repression of *manX*. Additional complementarity between SgrS and *manX* is predicted to encompass codons 4–7, though this region was not protected in footprints and mutations that would disrupt these interactions did not affect SgrS regulation of *manX'–'lacZ* (Figure 3E). Bouvier *et al*. (46) reported that base pairing within the first five codons of an mRNA coding sequence can inhibit translation through direct occlusion of ribosome binding. Although the experimentally confirmed pairing for SgrS and *manX* mRNA falls outside this window, *manX'–'lacZ* translational regulation by SgrS did not require degradation via the RNase E degradosome (Figure 5) suggesting that translational inhibition of *manX* is the primary mechanism of regulation. It is possible that other base pairing interactions not evident in footprints occur *in vivo* and contribute to a ribosome occlusion mechanism of translational inhibition. If this is the case, destabilization of the full-length *manXYZ* mRNA may be caused by polarity resulting from translational repression at *manX*. Microarrays that identified putative targets of the sRNA RyhB suggest that RyhB carries out a similar type of regulation on other operons (47).

In northern blots using a *manY*-specific probe, two bands appeared. The first was the size expected for the full-length *manXYZ* transcript, and the second was the size of *manYZ* mRNA. The second band did not appear in blots using a *manX*-specific probe, consistent with the idea that it was a *manYZ* transcript. Furthermore, 5′ RACE analysis identified a transcript with a processed 5′-end in the *manX–manY* intergenic region. Our 5′ RACE results and a *manY'–lacZ* transcriptional fusion (data not shown) were both consistent with the idea that *manYZ* is processed from the full-length *manXYZ* transcript. Northern blots show that the processing of *manYZ* is SgrS-independent since the *manYZ* transcript is observed in both wild-type and Δ*sgrS* mutants. Interestingly, analysis of the RNA extracted from *rne131* mutants showed that degradosome assembly on RNase E is involved in the processing (Figure 5B). Degradosome assembly is also required for RNase E-mediated turnover of SgrS–*ptsG* mRNA and SgrS–*manX* mRNA turnover [Figure 5A and B; and (12)]. RNase E catalytic activity (but not degradosome assembly) is required for processing of RNAs like rRNAs and tRNAs (48–50). The apparent involvement of the degradosome in generating the *manYZ* species may be somewhat unique. It remains to be seen whether the *manYZ* transcript is translated and what physiological function the processing serves.

A previous study suggested that one parameter affecting SgrS regulation of *ptsG* mRNA is the translational efficiency of *ptsG*. The translation rate is apparently reduced by co-translational membrane localization of the *ptsG* mRNA via SRP-dependent membrane insertion of nascent PtsG protein. Increased translational efficiency of *ptsG* greatly reduced SgrS's ability to downregulate *ptsG* translation (36). These observations prompted us to look at how translational efficiency of *manX* impacts SgrS regulation. We noticed that the GTG start codon of *manX* was highly conserved among different species (data not shown). GTG is a weaker start codon with decreased translational efficiency compared to ATG. Changing the GTG start codon of *manX* to an ATG increased activity of the *manX'–'lacZ* fusion but did not influence regulation by SgrS (Supplementary Figure S3), suggesting that at least this factor affecting the translational efficiency of *manX* does not play a role in its regulation by SgrS. Our experiments also demonstrated that membrane localization is not required for *manX* regulation, since our *manX'–'lacZ* fusions were regulated in the absence of the transmembrane segment coding sequences of *manY* and *manZ* (Figure 1). These data are consistent with the idea that although a small RNA can have multiple targets, the mechanisms by which it regulates each one may be different.

In addition to mannose, the ManX, ManY and ManZ proteins are capable of transporting numerous sugars including mannose, glucose, 2DG, αMG, fructose, glucosamine, *N*-acetylglucosamine and trehalose (17). We demonstrated that SgrS expression is induced in response to growth on two different glucose analogs: α-methylglucoside (αMG) and 2-deoxyglucose (2DG) (Figure 6). Analysis of *ptsG* mutants, *manXYZ* mutants and double mutants demonstrated that SgrS expression is induced in the absence of *ptsG* by both glucose analogs. Both EIICB^{Glc} (encoded by *ptsG*) and EII^{Man} (encoded by *manXYZ*) contribute to stress induction in the presence of αMG, though EIICB^{Glc} clearly plays the dominant role. In contrast, a functional EII^{Man} is required for induction of the stress by 2DG (Figure 6). These results indicated regulation of *manXYZ* is important under specific growth conditions where sugar–phosphates accumulate and further suggests that there may be more conditions that induce glucose–phosphate stress that have yet to be determined.

Computational and experimental analyses of different SgrS orthologs revealed that regulation of *ptsG* by SgrS is likely to be universally conserved in enteric species possessing SgrS (15,45). In contrast, we noted that the region of SgrS important for regulating *manX* in *E. coli* is not very highly conserved (data not shown), and our experiments indicate that SgrS orthologs from *E. carotovora* and *Y. pestis* do not regulate their cognate *manX* orthologs

(Figure 7). The fact that SgrS regulation of *manX* is not as conserved as regulation of *ptsG* implies that in at least some enterobacterial species, the major source of sugar–phosphates that cause stress is PtsG (EIICB^{Glc}) and not ManXYZ (EII^{Man}). The true nature of glucose–phosphate stress including the cellular targets and pathways affected is still mysterious. However, this study provides additional evidence that PTS-mediated transport of sugars and their subsequent metabolism are at the center of the stress.

SUPPLEMENTARY DATA

Supplementary Data are available at NAR Online.

ACKNOWLEDGEMENTS

FUNDING

REFERENCES

1. Waters,L.S. and Storz,G. (2009) Regulatory RNAs in bacteria. *Cell*, **136**, 615–628.
2. Storz,G., Opdyke,J.A. and Zhang,A. (2004) Controlling mRNA stability and translation with small, noncoding RNAs. *Curr. Opin. Microbiol.*, **7**, 140–144.
3. Sharma,C., Darfeuille,F., Plantinga,T. and Vogel,J. (2007) A small RNA regulates multiple ABC transporter mRNAs by targeting C/A-rich elements inside and upstream of ribosome-binding sites. *Genes & Dev.*, **21**, 2804–2817.
4. Pfeiffer,V., Papenfort,K., Lucchini,S., Hinton,J.C. and Vogel,J. (2009) Coding sequence targeting by MicC RNA reveals bacterial mRNA silencing downstream of translational initiation. *Nat. Struct. Mol. Biol.*, **16**, 840–846.
5. Desnoyers,G., Morissette,A., Prevost,K. and Masse,E. (2009) Small RNA-induced differential degradation of the polycistronic mRNA iscRSUA. *EMBO J.*, **28**, 1551–1561.
6. Møller,T., Franch,T., Udesen,C., Gerdes,K. and Valentin-Hansen,P. (2002) Spot 42 RNA mediates discoordinate expression of the *E. coli* galactose operon. *Genes Dev.*, **16**, 1696–1706.
7. Bohn,C., Rigoulay,C., Chabelskaya,S., Sharma,C.M., Marchais,A., Skorski,P., Borezee-Durant,E., Barbet,R., Jacquet,E., Jacq,A. *et al.* (2010) Experimental discovery of small RNAs in *Staphylococcus aureus* reveals a riboregulator of central metabolism. *Nucleic Acids Res.*, **38**, 6620–6636.
8. Vanderpool,C.K. (2007) Physiological consequences of small RNA-mediated regulation of glucose-phosphate stress. *Curr. Opin. Microbiol.*, **10**, 146–151.
9. Vanderpool,C.K. and Gottesman,S. (2004) Involvement of a novel transcriptional activator and small RNA in post-transcriptional regulation of the glucose phosphoenolpyruvate phosphotransferase system. *Mol. Microbiol.*, **54**, 1076–1089.
10. Kimata,K., Tanaka,Y., Inada,T. and Aiba,H. (2001) Expression of the glucose transporter gene, *ptsG*, is regulated at the mRNA degradation step in response to glycolytic flux in *Escherichia coli*. *EMBO J.*, **20**, 3587–3595.
11. Kawamoto,H., Koide,Y., Morita,T. and Aiba,H. (2006) Base-pairing requirement for RNA silencing by a bacterial small RNA and acceleration of duplex formation by Hfq. *Mol. Microbiol.*, **61**, 1013–1022.
12. Morita,T., Mochizuki,Y. and Aiba,H. (2006) Translational repression is sufficient for gene silencing by bacterial small noncoding RNAs in the absence of mRNA destruction. *Proc. Natl Acad. Sci. USA*, **103**, 4858–4863.
13. Morita,T., Maki,K. and Aiba,H. (2005) RNase E-based ribonucleoprotein complexes: mechanical basis of mRNA destabilization mediated by bacterial noncoding RNAs. *Genes Dev.*, **19**, 2176–2186.
14. Wadler,C.S. and Vanderpool,C.K. (2007) A dual function for a bacterial small RNA: SgrS performs base pairing-dependent regulation and encodes a functional polypeptide. *Proc. Natl Acad. Sci. USA*, **104**, 20454–20459.
15. Wadler,C.S. and Vanderpool,C.K. (2009) Characterization of homologs of the small RNA SgrS reveals diversity in function. *Nucleic Acids Res.*, **37**, 5477–5485.
16. Elliott,J. and Arber,W. (1978) *E. coli* K-12 *pel* mutants, which block phage lambda DNA injection, coincide with *ptsM*, which determines a component of a sugar transport system. *Mol. Gen. Genet.*, **161**, 1–8.
17. Meadow,N.D., Fox,D.K. and Roseman,S. (1990) The bacterial phosphoenolpyruvate: glycose phosphotransferase system. *Annu. Rev. Biochem.*, **59**, 497–542.
18. Erni,B., Zanolari,B. and Kocher,H.P. (1987) The mannose permease of *Escherichia coli* consists of three different proteins. Amino acid sequence and function in sugar transport, sugar phosphorylation, and penetration of phage lambda DNA. *J. Biol. Chem.*, **262**, 5238–5247.
19. Plumbridge,J. (1998) Control of the expression of the *manXYZ* operon in *Escherichia coli*: Mlc is a negative regulator of the mannose PTS. *Mol. Microbiol.*, **27**, 369–380.
20. Plumbridge,J. (2001) Regulation of PTS gene expression by the homologous transcriptional regulators, Mlc and NagC, in *Escherichia coli* (or how two similar repressors can behave differently). *J. Mol. Microbiol. Biotechnol.*, **3**, 371–380.
21. Yu,D.G., Ellis,H.M., Lee,E.C., Jenkins,N.A., Copeland,N.G. and Court,D.L. (2000) An efficient recombination system for chromosome engineering in *Escherichia coli*. *Proc. Natl Acad. Sci. USA*, **97**, 5978–5983.
22. Ellermeier,C.D., Janakiraman,A. and Slauch,J.M. (2002) Construction of targeted single copy *lac* fusions using lambda Red and FLP-mediated site-specific recombination in bacteria. *Gene*, **290**, 153–161.
23. Miller,J.H. (1972) *Experiments in Bacterial Genetics*. Cold Spring Harbor Laboratory, Cold Spring Harbor, New York.
24. Aiba,H., Adhya,S. and de Crombrugghe,B. (1981) Evidence for two functional *gal* promoters in intact *Escherichia coli* cells. *J. Biol. Chem.*, **256**, 11905–11910.
25. Majdalani,N., Chen,S., Murrow,J., St. John,K. and Gottesman,S. (2001) Regulation of RpoS by a novel small RNA: the characterization of RprA. *Mol. Microbiol.*, **39**, 1382–1394.
26. Argaman,L., Hershberg,R., Vogel,J., Bejerano,G., Wagner,E.G., Margalit,H. and Altuvia,S. (2001) Novel small RNA-encoding genes in the intergenic regions of *Escherichia coli*. *Curr. Biol.*, **11**, 941–950.

27. Zuker,M. (2003) Mfold web server for nucleic acid folding and hybridization prediction. *Nucleic Acids Res.*, **31**, 3406–3415.

28. Jensen,P.R. and Hammer,K. (1998) The sequence of spacers between the consensus sequences modulates the strength of prokaryotic promoters. *Appl. Environ. Microbiol.*, **64**, 82–87.

29. McDowall,K.J., Lin-Chao,S. and Cohen,S.N. (1994) A+U content rather than a particular nucleotide order determines the specificity of RNase E cleavage. *J. Biol. Chem.*, **269**, 10790–10796.

30. Mackie,G.A. (1991) Specific endonucleolytic cleavage of the mRNA for ribosomal protein S20 of *Escherichia coli* requires the product of the ams gene in vivo and in vitro. *J. Bacteriol.*, **173**, 2488–2497.

31. Mackie,G.A. (1992) Secondary structure of the mRNA for ribosomal protein S20. Implications for cleavage by ribonuclease E. *J. Biol. Chem.*, **267**, 1054–1061.

32. Majdalani,N., Cunning,C., Sledjeski,D., Elliott,T. and Gottesman,S. (1998) DsrA RNA regulates translation of RpoS message by an anti-antisense mechanism, independent of its action as an antisilencer of transcription. *Proc. Natl Acad. Sci. USA*, **95**, 12462–12467.

33. Guillier,M. and Gottesman,S. (2008) The 5′ end of two redundant sRNAs is involved in the regulation of multiple targets, including their own regulator. *Nucleic Acids Res.*, **36**, 6781–6794.

34. Massé,E., Escorcia,F.E. and Gottesman,S. (2003) Coupled degradation of a small regulatory RNA and its mRNA targets in *Escherichia coli. Genes Dev.*, **17**, 2374–2383.

35. Morita,T., Kawamoto,H., Mizota,T., Inada,T. and Aiba,H. (2004) Enolase in the RNA degradosome plays a crucial role in the rapid decay of glucose transporter mRNA in the response to phosphosugar stress in *Escherichia coli. Mol. Microbiol.*, **54**, 1063–1075.

36. Kawamoto,H., Morita,T., Shimizu,A., Inada,T. and Aiba,H. (2005) Implication of membrane localization of target mRNA in the action of a small RNA: mechanism of post-transcriptional regulation of glucose transporter in *Escherichia coli. Genes Dev.*, **19**, 328–338.

37. Reddy,P., Peterkofsky,A. and McKenney,K. (1985) Translational efficiency of the *Escherichia coli* adenylate cyclase gene: mutating the UUG initiation codon to GUG or AUG results in increased gene expression. *Proc. Natl Acad. Sci. USA*, **82**, 5656–5660.

38. Morita,T., El-Kazzaz,W., Tanaka,Y., Inada,T. and Aiba,H. (2003) Accumulation of glucose 6-phosphate or fructose 6-phosphate is responsible for destabilization of glucose transporter mRNA in *Escherichia coli. J. Biol. Chem.*, **278**, 15608–15614.

39. Amaral,D. and Kornberg,H.L. (1975) Regulation of fructose uptake by glucose in *Escherichia coli. J. Gen. Microbiol.*, **90**, 157–168.

40. Henderson,P.J., Giddens,R.A. and Jones-Mortimer,M.C. (1977) Transport of galactose, glucose and their molecular analogues by *Escherichia coli* K12. *Biochem. J.*, **162**, 309–320.

41. Curtis,S.J. and Epstein,W. (1975) Phosphorylation of D-glucose in *Escherichia coli* mutants defective in glucosephotransferase, mannosephotransferase, and glucokinase. *J. Bacteriol.*, **122**, 1189–1199.

42. Stock,J.B., Waygood,E.B., Meadow,N.D., Postma,P.W. and Roseman,S. (1982) Sugar transport by the bacterial phosphotransferase system. The glucose receptors of the *Salmonella typhimurium* phosphotransferase system. *J. Biol. Chem.*, **257**, 14543–14552.

43. Rephaeli,A.W. and Saier,M.H. Jr (1980) Substrate specificity and kinetic characterization of sugar uptake and phosphorylation, catalyzed by the mannose enzyme II of the phosphotransferase system in *Salmonella typhimurium. J. Biol. Chem.*, **255**, 8585–8591.

44. Kadner,R.J., Murphy,G.P. and Stephens,C.M. (1992) Two mechanisms for growth inhibition by elevated transport of sugar phosphates in *Escherichia coli. J. Gen. Microbiol.*, **138(Pt 10)**, 2007–2014.

45. Horler,R.S. and Vanderpool,C.K. (2009) Homologs of the small RNA SgrS are broadly distributed in enteric bacteria but have diverged in size and sequence. *Nucleic Acids Res.*, **37**, 5465–5476.

46. Bouvier,M., Sharma,C.M., Mika,F., Nierhaus,K.H. and Vogel,J. (2008) Small RNA binding to 5′ mRNA coding region inhibits translational initiation. *Mol. Cell*, **32**, 827–837.

47. Massé,E., Vanderpool,C.K. and Gottesman,S. (2005) Effect of RyhB small RNA on global iron use in *Escherichia coli. J. Bacteriol.*, **187**, 6962–6971.

48. Li,Z. and Deutscher,M.P. (2002) RNase E plays an essential role in the maturation of *Escherichia coli* tRNA precursors. *RNA*, **8**, 97–109.

49. Lopez,P.J., Marchand,I., Joyce,S.A. and Dreyfus,M. (1999) The C-terminal half of RNase E, which organizes the *Escherichia coli* degradosome, participates in mRNA degradation but not rRNA processing in vivo. *Mol. Microbiol.*, **33**, 188–199.

50. Ow,M.C., Liu,Q. and Kushner,S.R. (2000) Analysis of mRNA decay and rRNA processing in *Escherichia coli* in the absence of RNAse E-based degradosome assembly. *Mol. Microbiol.*, **38**, 854–866.